Metabolic flexibility via mitochondrial BCAA carrier SLC25A44 is required for optimal fever

Takeshi Yoneshiro[1,2], Naoya Kataoka[3], Jacquelyn M. Walejko[4], Kenji Ikeda[1,5], Zachary Brown[1], Momoko Yoneshiro[1,2], Scott B. Crown[4], Robert W. McGarrah[4,6], Phillip J. White[4,7], Kazuhiro Nakamura[3], and Shingo Kajimura[1,8,9]

[1] Diabetes Center and Department of Cell and Tissue Biology, University of California, San Francisco, CA, USA

[2] Division of Metabolic Medicine, Research Center for Advanced Science and Technology, the University of Tokyo, Tokyo, Japan.

[3] Department of Integrative Physiology, Nagoya University Graduate School of Medicine, Nagoya, Japan

[4] Duke Molecular Physiology Institute, Duke University School of Medicine, NC, USA

[5] Department of Molecular Endocrinology and Metabolism, Tokyo Medical and Dental University, Tokyo, Japan

[6] Department of Medicine, Division of Cardiology, Duke University School of Medicine, NC, USA

[7] Department of Medicine, Division of Endocrinology, Metabolism and Nutrition, Duke University School of Medicine, NC, USA

[8] Division of Endocrinology, Diabetes and Metabolism, Beth Israel Deaconess Medical Center, Harvard Medical School, MA, USA

[9] Corresponding Author: skajimur@bidmc.harvard.edu

ABSTRACT

Importing necessary metabolites into the mitochondrial matrix is a crucial step of fuel choice during stress adaptation. Branched chain-amino acids (BCAA, Valine, Leucine, and Isoleucine) are essential for anabolic processes like protein synthesis, but they are also imported into the mitochondria for catabolic reactions. What controls the distinct subcellular BCAA utilization during stress adaptation is insufficiently understood. The present study reports the role of SLC25A44, a recently identified mitochondrial BCAA carrier (MBC), in the regulation of mitochondrial BCAA catabolism and adaptive response to fever. We found that mitochondrial BCAA oxidation in brown adipose tissue (BAT) is significantly enhanced during fever in response to the pyrogenic mediator prostaglandin E_2 (PGE_2) and psychological stress. Genetic deletion of MBC in a BAT-specific manner blunts mitochondrial BCAA oxidation and non-shivering thermogenesis following intracerebroventricular PGE_2 administration. At a cellular level, MBC is required for mitochondrial BCAA deamination as well as the synthesis of mitochondrial amino acids and TCA intermediates. Together, these results illuminate the role of MBC as a determinant of metabolic flexibility to mitochondrial BCAA catabolism and optimal febrile responses. This study also offers an opportunity to control fever by rewiring the subcellular BCAA fate.

Keywords: Metabolic flexibility, BCAA, Brown adipose tissue, Mitochondrial transporter, MBC, Fever

INTRODUCTION

Eukaryotic cells utilize metabolites in distinct organelles during adaptation to stress. Such adaptive mechanisms provide another layer of flexibility in metabolite utilization, *a.k.a.,* metabolic flexibility, thereby allowing for robust adaptive fitness to stress. For example, leucine is a branched-chain amino acid (BCAA) that is used for anabolic processes, including protein synthesis and nutrition sensing via mTOR activation; however, leucine is also imported into the mitochondrial matrix for catabolic processes in metabolic organs, such as skeletal muscle and brown adipose tissue (BAT) upon exercise and cold adaptation, respectively (Neinast et al., 2019a, Lynch and Adams, 2014). The factors controlling the subcellular metabolite utilization, *e.g.,* the anabolic vs. catabolic responses to BCAA, during stress adaptation remains poorly understood.

One of the key determinants for subcellular metabolite utilization is mitochondrial carrier proteins. In contrast to the outer membrane which is comparatively permeable, the mitochondrial inner-membrane is impermeable. Accordingly, a variety of carrier proteins in the mitochondrial inner-membrane play pivotal roles in the regulation of metabolite delivery into the mitochondrial matrix. For instance, mitochondrial pyruvate carrier proteins (MPC1 and MPC2) are responsible for importing pyruvate into the matrix (Bricker et al., 2012, Herzig et al., 2012). Loss of MPC leads to reduced pyruvate oxidation, thereby shifting cellular metabolism toward glycolysis, *a.k.a.,* the Warburg effect, whereas ectopic expression of MPC1/2 promotes mitochondrial pyruvate oxidation via pyruvate dehydrogenase (PDH) (Schell et al., 2014, Vacanti et al., 2014). Of note, mitochondrial pyruvate uptake via MPC is essential for optimal adaptation to cold environment because genetic loss of MPC1 reduces glucose oxidation and TCA intermediates in brown adipocytes, leading to impaired BAT thermogenesis and cold tolerance in mice (Panic et al., 2020).

We recently identified SLC25A44 as a mitochondrial BCAA carrier (MBC) that is required for mitochondrial BCAA import and subsequent oxidation of BCAA in the matrix (Yoneshiro et al., 2019). CRISPRi-mediated depletion of *Slc25a44* decreases mitochondrial BCAA oxidation, thereby attenuating systemic BCAA clearance and cold tolerance in mice (Yoneshiro et al., 2019). A limitation of the previous study, however, is that MBC is widely expressed in the brain, skeletal muscle, and BAT, and thus, the tissue-specific contribution of MBC remains unknown. Accordingly, the present study generated the BAT-specific MBC knock-out (KO) mice and rigorously determined the extent to which mitochondrial BCAA catabolism *via* MBC is required for thermogenesis and metabolic adaptation to fever.

Fever is a physiological response to pyrogens, and in general, associated with a survival benefit. However, prolonged thermogenesis that chronically exceeds heat loss, such as psychological stress-induced hyperthermia, malignant hyperthermia, brain injury-induced fever, and endocrine fever, is deleterious and can cause widespread damage at cellular and organismal levels (Walter et al., 2016, Evans et al., 2015). Although recent studies uncovered the central neural circuits that control fever in response to pyrogens and psychological stress (Morrison and Nakamura, 2019), cellular and molecular mechanisms of febrile responses in peripheral organs are insufficiently understood. Hence, better understandings of the fever-associated metabolic adaptation may offer an effective intervention to soothe persistent fever.

Here, we report that mitochondrial BCAA oxidation in BAT is significantly enhanced during fever triggered by prostaglandin E_2 (PGE_2) and psychological stress. Mitochondrial BCAA uptake via MBC is crucial for cellular metabolic flexibility to catabolize BCAA in the mitochondria: BAT-specific MBC loss blunts mitochondrial BCAA catabolism and PGE_2-induced fever in mice. Mechanistically, mitochondrial BCAA uptake *via* MBC is crucial for the synthesis of

mitochondrial amino acids and TCA intermediates. Together, the present study provides new insights into the molecular mechanism by which mitochondrial BCAA transport via MBC regulates metabolic flexibility to BCAA catabolism and adaptive fitness to fever.

RESULTS

Fever promotes BCAA oxidation in BAT.

We developed an *in-vivo* monitoring system that allowed us to simultaneously record temperature changes in the body core and peripheral tissues of mice in response to thermogenic stimuli (**Fig.1A, B**). As a stimulus of fever, we used intracerebroventricular (ICV) administration of PGE_2: PGE_2 is a well-established pyrogenic mediator that binds to the EP3 subtype of its receptor in the preoptic area (POA) and triggers the pyrogenic circuit mechanism for the stimulation of sympathetic nerve activity likely by inhibiting thermoregulatory warm-sensitive POA neurons (Nakamura and Morrison, 2011, Nakamura, 2011). An ICV administration of PGE_2 into the POA sufficiently stimulates the non-shivering thermogenesis in BAT without altering the afferent signaling to the POA in rats (Nakamura et al., 2002, Nakamura and Morrison, 2008). Indicating the importance of the PGE_2-mediated signaling in infection-induced fever, EP3 receptor knockout mice fail to develop fever in response to intraperitoneal (i.p.) injection of lipopolysaccharide (LPS), an experimental model of systemic bacterial infection (Ushikubi et al., 1998, Lazarus et al., 2007).

Consistent with previous results (Nakamura et al., 2002), an ICV administration of PGE_2 (1.4 μg/mouse) rapidly increased the interscapular BAT (iBAT) temperature within 1–2 min following the administration (**Fig.1C**). This elevation of iBAT temperature was seen selectively to PGE_2 but not due to the technical artifact of ICV injection because iBAT temperature was not increased by an ICV administration of saline. The increase in iBAT temperature was followed by a significant

increase in core body (rectal) temperature by approximately 2 °C (average core body temperature rose to 38.8 °C) with a delay of 1–2 min, suggesting that the iBAT is a major heat source for the development of PGE_2-induced fever. Of note, chronic treatment with PGE_2 analog or ectopic expression of cyclooxygenase (COX) 2, a rate-limiting enzyme in prostaglandin synthesis, promotes beige fat biogenesis in the inguinal WAT (Vegiopoulos et al., 2010, Madsen et al., 2010). In contrast, the present study employed central administration of PGE_2 to acutely provoke febrile responses, and thus, PGE_2-induced browning of WAT was negligible in this context unless mice were acclimated to cold prior to PGE_2 administration (see Fig.2). Following the PGE_2-induced fever response, plasma levels of BCAA were significantly reduced, whereas no significant change was seen after saline administration (**Fig.1D**). Importantly, this reduction in plasma BCAA levels was accompanied by a significant increase in Val oxidation in the BAT (**Fig.1E**). This observation is consistent with our previous finding that cold-induced thermogenesis stimulates BCAA uptake in BAT and systemic BCAA clearance (Yoneshiro et al., 2019).

It is worth noting that the increase in BCAA oxidation in BAT is not specific to ICV administration of PGE_2 into mice. Psychological stress-induced hyperthermia is another physiological febrile response in which social-defeat stress stimulates excitatory neurotransmission from a ventromedial prefrontal cortical site to the dorsomedial hypothalamus, leading to activation of BAT thermogenesis and stress-induced hyperthermia in rats (Kataoka et al., 2020). The role of BAT thermogenesis in psychological stress has been reported in humans (Robinson et al., 2016). Following social-defeat stress in rats, we observed a significant increase in BCAA oxidation in the iBAT of rats under stress (**Fig.1F**). These results suggest that BCAA oxidation and thermogenesis in the BAT are induced during the development of fever triggered by PGE_2 and psychological stress.

Mitochondrial BCAA catabolism enhances PGE_2-induced fever.

Cold exposure and the subsequent activation of β_3-adrenoceptor (AR) signaling potently stimulates BAT thermogenesis (Collins, 2011). Analyses of the public available data of cold acclimated mice (GSE51080) found that chronic adaptation to 15 °C for two weeks potently stimulates the mitochondrial BCAA catabolic pathway, including the expression of Branched Chain Keto Acid Dehydrogenase E1 Subunit Alpha (BCKDHA), Dihydrolipoamide Branched Chain Transacylase (DBT), and the mitochondrial BCAA carrier *Slc25a44* (MBC), as well as the expression of BAT thermogenic genes, such as *Ucp1* and *Ppargc1a* (**Fig.2A**). Similarly, chronic administration of a β_3-AR agonist (CL-316,243, 0.1 mg/kg/day) for 7 days significantly activated the mitochondrial BCAA oxidation pathway in the BAT (**Fig.2B**).

Under these conditions of enhanced mitochondria BCAA oxidation, the PGE_2-induced febrile response was significantly potentiated. This enhanced thermogenesis in BAT was accompanied by higher rectal temperature and inguinal WAT temperature following PGE_2 injection (**Fig.2C, D**). In BAT, both cold acclimation and CL-316,243 administration significantly increased total heat production (Δ°C x min), maximum temperature (T_{max}), and the velocity of tissue temperature change (°C min^{-1}) in response to an ICV administration of PGE_2 (**Fig.2E**).

Mitochondrial BCAA carrier SLC25A44 is required for PGE_2-induced fever.

We next determined the extent to which mitochondrial BCAA entry via MBC/*Slc25a44* is required for PGE_2-induced febrile response. To this end, we first generated *Slc25a44* floxed mice and then crossed them with *Ucp1*-Cre mice to generate BAT-specific MBC KO mice (*Ucp1*-Cre x $Slc25a44^{flox/flox}$) and littermate control mice ($Slc25a44^{flox/flox}$) (**Fig.3A, B, Fig.S1A**). On a regular chow diet, BAT-specific MBC deletion did not alter body weight and tissue mass of metabolic

organs, including the BAT, liver, WAT, and skeletal muscle (**Fig.3C, Fig.S1B, C**). Morphologically, we found no major difference in brown adipocytes of BAT-specific MBC KO mice (**Fig.3D, Fig.S1D**). The phenotype is consistent with our previous study in which neither CRISPRi-mediated knockdown of MBC nor BAT-specific deletion of BCKDHA altered brown adipocyte differentiation (Yoneshiro et al., 2019). However, MBC loss significantly reduced Valine oxidation in the BAT, but not in the skeletal muscle (**Fig.3E**), reinforcing the requirement of MBC for mitochondrial BCAA oxidation *in vivo*.

When PGE_2 was administered to the BAT-specific MBC KO mice under ambient temperature, we found that PGE_2-induced febrile response was substantially attenuated relative to control mice (**Fig.3F, G**). Specifically, total heat production (Δ°C x min) and maximum temperature (T_{max}) were significantly lower in BAT-specific MBC KO mice than those in control mice (**Fig.3H, I**). Of note, we observed no difference in the velocity of the initial rise in iBAT temperature (°C min^{-1}) for the first five minutes after PGE_2 administration between the two groups (**Fig.3J**). The data suggest that mitochondrial BCAA uptake via MBC is required for sustaining thermogenic activity in BAT, while it is dispensable for the initiation of thermogenesis following PGE_2 administration.

Mitochondrial BCAA catabolism controls PGE_2-induced thermogenesis via UCP1-dependent and UCP1-independent mechanisms.

To test if the above phenotype of BAT-specific MBC KO mice is due to reduced BCAA oxidation, we next examined the extent to which genetic loss of BCKDHA, a mitochondria-localized BCAA oxidation enzyme, affects the PGE_2-induced febrile response. We previously reported that BAT-specific BCKDHA KO mice (*Ucp1*-Cre x *Bckdha*$^{flox/flox}$) exhibited impaired BCAA oxidation, systemic BCAA clearance, and thermogenesis in BAT (Yoneshiro et al., 2019). Consistent with

the phenotype seen in BAT-specific MBC KO mice, we found that PGE_2-induced BAT thermogenesis was attenuated in the BAT-specific BCKDHA KO mice relative to control mice (**Fig.4A**). It is notable that total heat production (Δ°C x min) and maximum temperature (T_{max}) in the BAT were significantly lower in the BCKDHA KO mice than those in control mice (**Fig.4B, C**), whereas no difference was seen in the velocity of the initial BAT temperature change (°C min^{-1}) between the genotypes (**Fig.4D**). These results further support the view that mitochondrial BCAA catabolism through the actions of MBC and BCKDH is required for the maintenance of PGE_2-induced BAT thermogenesis, but not required for the initiation of thermogenesis.

Cold-induced thermogenesis in iBAT requires UCP1 (Enerback et al., 1997). This UCP1-dependency in iBAT is attributed to the fact that brown adipocytes have a low ATP synthesis capacity (Kramarova et al., 2008), and thus, ATP-dependent (*i.e.,* UCP1-independent) futile cycle, such as Ca^{2+} cycling or creatine cycling (Ikeda et al., 2017, Kazak et al., 2015) may not compensate for the lack of UCP1. Nonetheless, several studies reported that UCP1 is dispensable for febrile responses to *i.p.* administration of LPS or interleukin (IL)-1β (Okamatsu-Ogura et al., 2007, Riley et al., 2016, Eskilsson et al., 2020). Accordingly, we examined if ICV administration of PGE_2 induces UCP1-dependent thermogenesis in iBAT. In mice kept under an ambient temperature condition, we found that PGE_2-induced thermogenesis was totally blunted in UCP1 KO mice (**Fig.4E**). The data are consistent with the result in cultured brown adipocytes in which BCAA supplementation enhanced norepinephrine-stimulated cellular respiration in an UCP1-dependent manner (**Fig.4F**). In contrast, BCAA supplementation in UCP1 KO beige adipocytes significantly enhanced norepinephrine-stimulated cellular respiration, although the effect was much less than that in WT beige adipocytes (WT: +46.4 ± 1.2%, UCP1 KO: +30.6 ± 2.5%, $P < 0.001$, **Fig.4G**).

Given our previous works on the mechanism of Ca^{2+} cycling thermogenesis via SERCA2 (Ikeda et al., 2017), we next determined the extent to which SERCA2-mediated Ca^{2+} cycling mediates BCAA catabolism and thermogenesis. To this end, we depleted SERCA2 (encoded by *Atp2a2*) using two independent shRNAs targeting *Atp2a2* in UCP1 null beige adipocytes (**Fig.4H**). In beige adipocytes, norepinephrine treatment significantly stimulated Val oxidation even in the absence of UCP1; however, the norepinephrine-induced BCAA oxidation was near completely blunted when SERCA2 was depleted (**Fig.4I**). Importantly, depletion of SERCA2 eliminated the stimulatory effect of BCAA supplementation on UCP1-independent respiration following norepinephrine treatment (**Fig.4J**). These results suggest that mitochondrial BCAA oxidation enhances thermogenesis in brown fat and beige fat through UCP1-dependent and independent mechanisms, respectively.

Metabolic flexibility to mitochondrial BCAA catabolism is required for sustained thermogenesis.

Fatty acids and glucose are considered to be the primary fuel for BAT thermogenesis, while the contribution of BCAA as a carbon fuel appears marginal even though BAT is a major metabolic-sink for BCAA (Yoneshiro et al., 2019, Lopez-Soriano et al., 1988, Neinast et al., 2019b, Hui et al., 2020). Nonetheless, our data raise the possibility that mitochondrial BCAA catabolism (*i.e.,* mitochondrial import, deamination, and oxidation) is needed for sustaining thermogenic activity even under conditions in which the primary fuels are not limited. To probe this, we cultured differentiated brown adipocytes in the presence of glucose at a physiological level (5 mM) and measured OCR in response to norepinephrine. Norepinephrine treatment rapidly increased OCR within 5-6 min, whereas this effect gradually declined. However, the supplementation of Leu after

norepinephrine effectively maintained the elevated levels of OCR (**Fig.5A**). On the other hand, such an stimulatory effect of Leu was completely lost in MBC KO brown adipocytes, although these cells were able to respond to norepinephrine and increased OCR (**Fig.5B**).

The effect of Leu supplementation on OCR is to potentiate the action of thermogenic stimuli: when Leu was supplemented in brown adipocytes prior to norepinephrine treatment, we observed no increase in OCR. However, norepinephrine-induced thermogenesis was significantly enhanced when Leu was supplemented even in the presence of high glucose at 20 mM (**Fig.5C**). Importantly, this effect of Leu was not seen in the absence of MBC (**Fig.5D**). In turn, MBC KO brown adipocytes produced higher levels of lactate than WT control cells following norepinephrine treatment (**Fig.5E**), suggesting that MBC KO cells are restricted to utilize glucose even in the presence of Leu.

MBC is required for the synthesis of the mitochondrial amino acid pool and TCA intermediates.

To address how MBC controls BCAA catabolism, we next performed uniformly ^{13}C-labeled, ^{15}N-labeled Leu ([U-$^{13}C_6$, $^{15}N_1$] Leu) tracing in differentiated brown adipocytes (**Fig.S2A**). As we previously reported (Yoneshiro et al., 2019), brown adipocytes dominantly express branched-chain amino acid aminotransferase 2 (BCAT2), the mitochondria-localized form of BCAT, and thus, deamination and oxidation of BCAA largely occur in the mitochondrial matrix (**Fig.6A**). GC-MS analysis of intercellular metabolites revealed that levels of Leu, α-ketoisocaproate (KIC), Ala, and Glu, were significantly lower in MBC KO brown adipocytes than those in WT control cells (**Fig.6B**). There was a trend towards lower Asp levels in MBC KO cells relative to WT control cells, although the difference was not statistically significant. This is likely because BAT expresses

very low levels of aspartate aminotransferase (GOT), the enzyme that catalyzes the conversion of oxaloacetate to Asp, whereas BAT expresses high levels of glutamate-pyruvate transaminase (GPT) that catalyzes the reversible conversion of Ala and α-ketoglutarate (α-KG) to Glu and pyruvate (**Fig.S2B**). Importantly, the reduced levels of KIC, Glu, and Ala in MBC KO cells were due to the reduced conversion from Leu because levels of labeled KIC, Glu, and Ala (*i.e.,* Leu-derived) were significantly lower in KO cells than those in WT control cells (**Fig.6C, D**). Also, there was a slight, but significant reduction in M3 labeled Asp in KO cells relative to control cells.

Following the deamination of Leu in the mitochondria, KIC fuels the TCA cycle in brown adipocytes. Our previous study showed that norepinephrine treatment significantly increased the Leu-derived TCA cycle intermediates (Yoneshiro et al., 2019). Consistent with this prior observation, we found that intracellular levels of α-KG, succinate, malate, and citrate increased after norepinephrine treatment; however, the increases in α-KG and malate levels occurred at significantly less degree in MBC KO cells (**Fig.6E**). Importantly, the total pool size of TCA cycle intermediates in MBC KO cells was smaller than that in WT control cells at 60 min after norepinephrine treatment (**Fig.6F**), although the differences were not seen at basal state (before norepinephrine treatment) (**Fig.S2C**). These results are likely relevant to the finding that mitochondrial BCAA catabolism is required for sustaining BAT thermogenesis, but not for the initial trigger of thermogenesis. Even under the reduced pool size, the contribution of Leu into the TCA cycle, as shown by ^{13}C ion counts and the mole percentage enrichment (MPE), was lower in MBC KO cells than that in WT control cells (**Fig.6G, H**).

Together, the present data suggest the following model (**Fig.7**). In response to febrile stimuli, such as increased PGE_2 or psychological stress, mitochondrial BCAA catabolism is activated along with

enhanced BAT thermogenesis. The sympathetically stimulated mitochondrial BCAA catabolism is required for maintaining active BAT thermogenesis to sustain febrile responses. Mechanistically, MBC is a critical gatekeeper of mitochondrial BCAA transport and subsequent catabolic reactions, including deamination as well as the synthesis of mitochondrial amino acid pool and TCA intermediates.

DISCUSSION

In general, hyperthermic responses to pyrogens are considered beneficial because the elevation of body temperature can prevent the replication of infective pathogens, while activating innate immunity (*e.g.,* enhanced cytokine release). However, persistent thermogenesis, often associated with psychological stress-induced hyperthermia, malignant hyperthermia, traumatic brain injury, and endocrine fever, causes severe exhaustion and, in the worst cases, it leads to widespread cellular and organ damage, such as renal injury, liver failure, and edema (Walter et al., 2016).

Fever involves multiple involuntary effector responses besides BAT thermogenesis, including skeletal muscle shivering and cutaneous vasoconstriction (Morrison and Nakamura, 2019). Hence, experimental setting, such as the types of pyrogen and anesthetizer would influence the data interpretation. For instance, UCP1 null mice exhibit fever in response to systemic administration (i.p. injection) of LPS or IL-1β under a non-anesthetized condition (Okamatsu-Ogura et al., 2007, Riley et al., 2016, Eskilsson et al., 2020). The difference from the present study is due to the fact that, under an ambient temperature, BAT thermogenesis can be compensated by involuntary (*e.g.*, shivering, vasoconstriction) and behavioral (*e.g.*, increased locomotion) responses until body temperature reaches to a set-point in the pyrogen-sensitized thermoregulatory circuitry of the brain (Nakamura, 2011, Morrison and Nakamura, 2019). On the other hand, the present temperature

recording in anesthetized mice excludes such responses, and specifically determines the contribution of non-shivering thermogenesis to febrile responses in response to the ICV administration of PGE_2.

Nonetheless, the present study demonstrates that mitochondrial BCAA catabolism plays a vital role in maintaining BAT thermogenesis to sustain febrile responses, and thus suggests a new opportunity to soothe persistent fever by blocking this pathway. Conversely, it is conceivable that enhancing BCAA catabolism is effective for elderly populations in which approximately 20-30% of the elderly show blunted or absent febrile response to pyrogens (Norman, 2000). It is worth noting that the thermogenic capacity of BAT is significantly attenuated in aging, and that this attenuation is closely coupled with reduced BCAA oxidation (Tajima et al., 2019). This age-associated attenuation in BCAA oxidation is attributed, in part, to reduced protein lipoylation in the E2 subunit of the BCKDH complex, while dietary supplementation of α-lipoic acids effectively restores the protein lipoylation of BCKDH and thermogenic function of BAT in old mice (Tajima et al., 2019). Since a blunted fever response to infections represents a poorer prognosis in the elderly (Norman, 2000), enhancing BCAA catabolism, *e.g.,* by α-lipoic acid supplementation or inhibition of BCKDH kinase activity (BDK, an inhibitory kinase of BCKDH), may represent effective means to alleviate age-associated decline in fever responses.

BCAAs are more than fuel in thermogenic fat: It has been well appreciated that lipolysis-derived fatty acids are the primary fuel for thermogenesis in brown and beige fat (Townsend and Tseng, 2014). Indeed, blockade of lipolysis in adipose tissues, by genetically deleting adipose triglyceride lipase (ATGL) or the ATGL-activating protein comparative gene identification-58 (CGI-58) in adipocytes, potently attenuates BAT thermogenesis in mice (Schreiber et al., 2017, Shin et al., 2017). On the other hand, the contribution of BCAA to the TCA cycle appears minor

relative to fatty acids or glucose in BAT (Hui et al., 2020), although BAT is a significant metabolic-sink for BCAA when activated (Yoneshiro et al., 2019, Lopez-Soriano et al., 1988, Neinast et al., 2019b). This is aligned with the present results that mitochondrial BCAA uptake and oxidation are required for the maintenance, rather than the initiation, of BAT thermogenesis (see Fig. 3 and 4). Presumably, BAT is able to initiate the rising phase of febrile thermogenesis by utilizing fatty acids and glucose even in the absence of BCAA.

We speculate the following possibilities as to why mitochondrial BCAA catabolism is required in BAT: The first possibility is the role of BCAA catabolic products as replenishment of TCA cycle intermediates. Complete oxidation of acetyl-CoA from β-oxidation requires the condensation of acetyl-CoA and oxaloacetate in the TCA cycle. Generation of the anaplerotic products from BCAA oxidation (see Fig. 6) may allow for sustaining fatty acid oxidation in the mitochondrial matrix. The second possibility is the role of BCAA-derived amino acids in the mitochondria. Given the role of BCAA as a major nitrogen donor, deamination of BCAA by BCAT2 is critical for the synthesis of Glu, Ala, and Asp. Indeed, loss of MBC leads to a reduction in these amino acids in brown adipocytes. Moreover, since thermogenic stimuli activate the purine and pyrimidine synthesis pathway in BAT (Lu et al., 2017), BCAA-derived nitrogen could contribute to nucleotide synthesis. Third, BCAA catabolism may promote *de novo* lipogenesis by generating monomethyl branched-chain fatty acids (mmBCFAs) as previously reported (Green et al., 2016, Wallace et al., 2018). BAT is a major site of mmBCFA synthesis in which the expression of mmBCFA synthesis enzymes, such as carnitine acetyltransferase (CrAT), is increased after one-month-cold acclimatization (Wallace et al., 2018). This pathway is activated during chronic cold adaptation (3 weeks and after) (Yoneshiro et al., 2019), and thus, BCAA may contribute to mmBCFA synthesis

under a cold-acclimated state. Together, the role of BCAA in thermogenic fat is likely more than merely a carbon source of fuel into the TCA cycle.

The role of mitochondrial carriers in metabolic flexibility: Metabolic flexibility is a term that often describes the ability of cells, organs, or an organism to shift the principal types of fuel in order to meet their metabolic demands in response to changes in external and internal conditions. A well-appreciated example is in the skeletal muscle upon exercise in which acute and high-intensity exercise utilizes glucose oxidation, while aerobic and endurance exercise triggers a fuel switch toward fatty acid oxidation (Smith et al., 2018, Goodpaster and Sparks, 2017). Importing necessary metabolites into the mitochondrial matrix (*e.g.,* acyl-CoA for fatty acids) is an essential step of metabolic flexibility: for instance, blockade of carnitine shuttle by deleting carnitine palmitoyltransferase 1 (CPT1) attenuates muscle function and endurance exercise capacity in mice (Wicks et al., 2015). It is pertinent to note that genetic mutations in carnitine-acylcarnitine translocase (encoded by *SLC25A20*), which mediates the transport of acylcarnitines into the mitochondrial matrix, causes severe metabolic disorders, including hypoglycemia, myopathy, and muscle weakness in humans (Fukushima et al., 2013, Iacobazzi et al., 2004).

In the present study, we found that when stimulated with norepinephrine, brown adipocytes lacking MBC/*Slc25a44* increase lactate production, suggesting a shift to glucose utilization. This metabolic inflexibility is accompanied by an impairment in sustained thermogenic activity in brown adipocytes. Recent studies in cardiomyocytes have demonstrated an interplay between BCAA and glucose oxidation (Li et al., 2017, Shao et al., 2018). The extent to which mitochondrial import of BCAA affects fuel selection in BAT in similar ways requires further study. Of particular note, impaired BCAA oxidation in peripheral metabolic organs and concomitant elevation of circulating BCAA levels are a metabolic signature of obesity, insulin resistance, and type 2

diabetes (Felig et al., 1969, Wang et al., 2011, Newgard et al., 2009, Wurtz et al., 2013). Quantitative BCAA tracing shows that reduced BCAA oxidation in the liver and adipose tissues re-distributes BCAA into the muscle, leading to BCAA overload and insulin resistance (Neinast et al., 2019b). Thus, future studies are needed to determine the role of MBC in the pathogenesis of insulin resistance.

Acknowledgments. We thank Olga Byakina for her technical support in the temperature recording. This work was supported by the NIH (DK097441, DK126160, DK125281 and DK127575 to S.K., 5K08HL135275 to R.W.M., and F32HL137398 to S.B.C), an American Diabetes Association Pathways to Stop Diabetes Initiator Award (# 1-16-INI-17) to P.J.W., the Edward Mallinckrodt, Jr. Foundation to S.K., MEXT KAKENHI (15H05932, 15K21744 and 20H03418 to K.N. and 19K06954 to N.K.), AMED (20gm5010002s0304) to K.N., and JST Moonshot R&D (JPMJMS2023) to K.N. T.Y. is supported by the JSPS Fellowships and the Uehara Memorial Foundation, and J.M.W. is supported by Cardiovascular-Metabolic Fellowship (#1-21-CMF-005).

Competing interests. The authors declare that they have no competing interests.

MATERIALS AND METHODS

Animals

All the animal experiments were performed following the guidelines by the UCSF Institutional Animal Care and Use Committee or by the Nagoya University Animal Experiment Committee, and approved by the committees. The wild type and UCP1 KO mice aged ~14 weeks had free access to food and water, 12-hour light cycles, and were caged at 23 °C. BAT-specific *Bckdha* KO mice were obtained by crossing *Bckdha* floxed mice with *Ucp1*-Cre mice, as reported previously (Yoneshiro et al., 2019). For the generation of BAT-specific *Slc25a44*/MBC KO mice (MBC^{UCP1} KO mice), *Slc25a44* floxed mice were obtained from the Applied StemCell (MC185, Milpitas, California, USA) and crossed with *Ucp1*-Cre mice. All mice were C57BL/6 background. Adult male Sprague-Dawley (SD) rats were housed two or three to a cage with ad libitum access to food and water in a room airconditioned at 24 °C with a standard 12-hour light/dark cycle.

Cold acclimatization and treatment with β_3 adrenergic receptor agonist

Wild type mice were acclimated to either thermoneutral temperature at 30 °C (n = 5) or cold temperature at 15 °C (n = 5) for 2 weeks and were used for temperature recording in fever response. UCP1 KO mice and the littermate wild type mice (control) were treated with saline (control n = 4, UCP1 KO n = 5) or 0.1 mg/kg/day of CL-316,243, β_3 adrenergic receptor agonist (control n = 5, UCP1 KO n = 6), for 1 week and were used for temperature recording in fever response.

Temperature recordings in febrile response

Mice under anesthesia with urethane (1.3 mg/kg) were positioned in a stereotaxic apparatus according to the mouse brain atlas (Franklin and Paxinos, 2008). A stainless-steel cannula (outer diameter, 0.35 mm) and a 1 ml disposable syringe were connected with polyethylene tubing and were inserted perpendicularly into the right lateral ventricle (coordinates: 0.1 mm posterior to bregma, 0.1 mm lateral to the midline, and 1 mm ventral to the brain surface). Then, mice were left on a self-regulating heating pad to stabilize the rectal temperature (T_{Rec}) at 37 °C and implanted with a type T thermocouple probe (IT-18, Physitemp, Clifton, New Jersey) in the rectum and with needle microprobes (MT-29/1, Physitemp) in the interscapular BAT and inguinal WAT (Yoneshiro et al., 2019). Tissue temperatures were simultaneously recorded by TC-2000 Meter (Sable Systems International). When tissue temperatures were stable, for > 5min, PGE_2 (1.4 μg;

Sigma) in 1.4 µl of pyrogen-free saline or only saline was injected into the ventricle through the cannula. The changes in tissue temperatures were contentiously measured every second for 1 hour or as indicated, and the mean value per minute was calculated.

Tissue histology. For hematoxylin and eosin (H&E) staining, tissues of mice were fixed in 4% paraformaldehyde overnight at 4 °C, followed by dehydration in 70% ethanol. After the dehydration procedure, tissues were embedded in paraffin, sectioned at a thickness of 5 µm, and stained with H&E following the standard protocol. Images of tissue samples were captured using the Inverted Microscope Leica DMi8.

BCAA oxidation

Isolated tissue (20-30 mg) was placed in a polypropylene round-bottom tube and incubated in the 1 mL KRB/HEPES buffer containing 0.16 µCi/ml [1-^{14}C] Val at 37 °C for 1 hour. After adding 350 µL of 30% hydrogen peroxide in the tube, [^{14}C] CO_2 was trapped in the center well supplemented with 300 µL of 1 M benzethonium hydroxide solution for 20 min at room temperature. BCAA oxidation was quantified by counting radioactivity of trapped [^{14}C] CO_2 using a scintillation counter.

Cell culture

Immortalized brown and beige adipocytes from C57BL/6 mice and UCP1 KO brown and beige adipocytes were generated in our previous studies (Yoneshiro et al., 2019, Ikeda et al., 2017). Adipocyte differentiation was induced by treating confluent preadipocytes with DMEM containing 10% FBS, 0.5 mM isobutylmethylxanthine, 125 nM indomethacin, 2 µg/ml dexamethasone, 850 nM insulin, 1 nM T3 and 0.5 µM rosiglitazone. Two days after induction, cells were switched to a maintenance medium containing 10% FBS, 850 nM insulin, 1 nM T3 and 0.5 µM rosiglitazone (Ohno et al., 2012). The cells were fully differentiated 6-7 days after inducing differentiation.

Generation of *Slc25a44*/MBC KO brown adipocytes

For the generation of *Slc25a44*/MBC KO brown adipocytes, preadipocytes isolated from BAT of *Slc25a44*$^{flox/flox}$ mice were immortalized by using the SV40 Large T antigen as described

previously (Yoneshiro et al., 2019) and subsequently infected with a retrovirus containing either empty vector or Cre (#34565, Addgene), followed by hygromycin selection at a dose of 200 μg/ml.

Cellular respiration

Oxygen consumption rate (OCR) in cultured adipocytes was measured using the Seahorse XFe Extracellular Flux Analyzer (Agilent) in a 24-well plate. For measurement of NE-induced respiration in the presence and absence of BCAA, differentiated adipocytes were maintained in KRB/HEPES buffer containing 20 or 5 mM glucose, 200 nM adenosine, and 2% BSA. During OCR measurement, cells were treated with 2 mM Val or vehicle, and subsequently treated with NE (1 μM) at the indicated time point.

Stable isotope-labeled leucine metabolome analysis. To determine the effect of MBC depletion on the metabolic fate of BCAA in brown adipocytes, we used [$^{13}C_6$, $^{15}N_1$] Leu tracing. Differentiated MBC KO or control brown adipocytes were incubated in the BCAA free medium supplemented with [$^{13}C_6$, $^{15}N_1$] Leu (608068, Sigma-Aldrich) and were harvested at 0, 0.5, and 1 hour after the treatment with norepinephrine. Metabolites were then extracted using by scraping cells in 3mL chilled 100% MeOH (LC-MC grade). The extracts were then centrifuged at 4 °C and 14400 x g for 10 min, and the clarified aqueous phase was transferred to a fresh Eppendorf and stored in -80 °C until processing for GC-MS analysis. For GC-MS analysis, 10 μL of 0.05 mM norvaline was added to 100 μL of extracted metabolites and dried under N_2 gas-flow at 37°C using an evaporator. Amino and organic acids were derivatized via methoximation and silylation. In brief, metabolites were resuspended in 25 μL of methoxylamine hydrochloride (2% (w/v) in pyridine) and incubated at 40 °C for 90 minutes on a heating block. After brief centrifugation, 35 μL of MTBSTFA + 1% TBDMS was added and the samples were incubated at 60 °C for 30 minutes. GC-MS analysis was performed on an Agilent 7890B GC system equipped with a HP-5MS capillary column connected to an Agilent 5977A Mass Spectrometer 50. Mass isotopomer distributions were obtained by integration of ion chromatograms 51 and corrected for natural isotope abundances Relative levels of metabolites or isotopomers were calculated by normalizing to norvaline. Mole percent enrichment (MPE) of isotopes, an index of isotopic enrichment of metabolites, was calculated as the percent of all atoms within the metabolite pool that are labeled according to the established formula (Wallace et al., 2018).

RNA preparation and quantitative RT-PCR. Total RNA was extracted from tissue or cells using RNeasy mini-kit (Qiagen), and cDNA was synthesized using iScript cDNA Synthesis kit (BioRad) according to the manufactural protocols. qRT-PCR was performed using an ABI ViiA™7 PCR cycler. The primer sequences are listed in **Supplementary Table 1**. The gene expression levels were normalized to internal control *36B4* levels (Yoneshiro et al., 2019).

Statistical analyses. All data were expressed as the means with SEMs and analyzed by using statistical software (SPSS 25.0; IBM Japan, Tokyo, Japan). Comparisons between the two groups were analyzed using the paired *t*-test or the Student's *t*-test, as appropriate. Analysis of variance (ANOVA) followed by Tukey's test was used for multiple-group comparisons. Two-way repeated-measures ANOVA was used for the comparisons of repeated measurements. Two-tailed *P* value ≤ 0.05 was considered as statistically significant.

REFERENCES

BRICKER, D. K., TAYLOR, E. B., SCHELL, J. C., ORSAK, T., BOUTRON, A., CHEN, Y. C., COX, J. E., CARDON, C. M., VAN VRANKEN, J. G., DEPHOURE, N., REDIN, C., BOUDINA, S., GYGI, S. P., BRIVET, M., THUMMEL, C. S. & RUTTER, J. 2012. A mitochondrial pyruvate carrier required for pyruvate uptake in yeast, Drosophila, and humans. *Science,* 337**,** 96-100.

COLLINS, S. 2011. beta-Adrenoceptor Signaling Networks in Adipocytes for Recruiting Stored Fat and Energy Expenditure. *Front Endocrinol (Lausanne),* 2**,** 102.

ENERBACK, S., JACOBSSON, A., SIMPSON, E. M., GUERRA, C., YAMASHITA, H., HARPER, M. E. & KOZAK, L. P. 1997. Mice lacking mitochondrial uncoupling protein are cold-sensitive but not obese. *Nature,* 387**,** 90-4.

ESKILSSON, A., SHIONOYA, K., ENERBACK, S., ENGBLOM, D. & BLOMQVIST, A. 2020. The generation of immune-induced fever and emotional stress-induced hyperthermia in mice does not involve brown adipose tissue thermogenesis. *FASEB J,* 34**,** 5863-5876.

EVANS, S. S., REPASKY, E. A. & FISHER, D. T. 2015. Fever and the thermal regulation of immunity: the immune system feels the heat. *Nat Rev Immunol,* 15**,** 335-49.

FELIG, P., MARLISS, E. & CAHILL, G. F., JR. 1969. Plasma amino acid levels and insulin secretion in obesity. *N Engl J Med,* 281**,** 811-6.

FRANKLIN, K. & PAXINOS, G. 2008. The Mouse Brain in Stereotaxic Coordinates, 3rd Edition.

FUKUSHIMA, T., KANEOKA, H., YASUNO, T., SASAGURI, Y., TOKUYASU, T., TOKORO, K., FUKAO, T. & SAITO, T. 2013. Three novel mutations in the carnitine-acylcarnitine translocase (CACT) gene in patients with CACT deficiency and in healthy individuals. *J Hum Genet,* 58**,** 788-93.

GOODPASTER, B. H. & SPARKS, L. M. 2017. Metabolic Flexibility in Health and Disease. *Cell Metab,* 25**,** 1027-1036.

GREEN, C. R., WALLACE, M., DIVAKARUNI, A. S., PHILLIPS, S. A., MURPHY, A. N., CIARALDI, T. P. & METALLO, C. M. 2016. Branched-chain amino acid catabolism fuels adipocyte differentiation and lipogenesis. *Nat Chem Biol,* 12**,** 15-21.

HERZIG, S., RAEMY, E., MONTESSUIT, S., VEUTHEY, J. L., ZAMBONI, N., WESTERMANN, B., KUNJI, E. R. & MARTINOU, J. C. 2012. Identification and functional expression of the mitochondrial pyruvate carrier. *Science,* 337**,** 93-6.

HUI, S., COWAN, A. J., ZENG, X., YANG, L., TESLAA, T., LI, X., BARTMAN, C., ZHANG, Z., JANG, C., WANG, L., LU, W., ROJAS, J., BAUR, J. & RABINOWITZ, J. D. 2020. Quantitative Fluxomics of Circulating Metabolites. *Cell Metab,* 32**,** 676-688 e4.

IACOBAZZI, V., INVERNIZZI, F., BARATTA, S., PONS, R., CHUNG, W., GARAVAGLIA, B., DIONISI-VICI, C., RIBES, A., PARINI, R., HUERTAS, M. D., ROLDAN, S., LAURIA, G., PALMIERI, F. & TARONI, F. 2004. Molecular and functional analysis of SLC25A20 mutations causing carnitine-acylcarnitine translocase deficiency. *Hum Mutat,* 24**,** 312-20.

IKEDA, K., KANG, Q., YONESHIRO, T., CAMPOREZ, J. P., MAKI, H., HOMMA, M., SHINODA, K., CHEN, Y., LU, X., MARETICH, P., TAJIMA, K., AJUWON, K. M., SOGA, T. & KAJIMURA, S. 2017. UCP1-independent signaling involving SERCA2b-mediated calcium cycling regulates beige fat thermogenesis and systemic glucose homeostasis. *Nat Med,* 23**,** 1454-1465.

KATAOKA, N., SHIMA, Y., NAKAJIMA, K. & NAKAMURA, K. 2020. A central master driver of psychosocial stress responses in the rat. *Science,* 367**,** 1105-1112.

KAZAK, L., CHOUCHANI, E. T., JEDRYCHOWSKI, M. P., ERICKSON, B. K., SHINODA, K., COHEN, P., VETRIVELAN, R., LU, G. Z., LAZNIK-BOGOSLAVSKI, D., HASENFUSS, S. C., KAJIMURA, S., GYGI, S. P. & SPIEGELMAN, B. M. 2015. A creatine-driven substrate cycle enhances energy expenditure and thermogenesis in beige fat. *Cell,* 163**,** 643-55.

KRAMAROVA, T. V., SHABALINA, I. G., ANDERSSON, U., WESTERBERG, R., CARLBERG, I., HOUSTEK, J., NEDERGAARD, J. & CANNON, B. 2008. Mitochondrial ATP synthase levels in brown adipose tissue are governed by the c-Fo subunit P1 isoform. *FASEB J,* 22**,** 55-63.

LAZARUS, M., YOSHIDA, K., COPPARI, R., BASS, C. E., MOCHIZUKI, T., LOWELL, B. B. & SAPER, C. B. 2007. EP3 prostaglandin receptors in the median preoptic nucleus are critical for fever responses. *Nat Neurosci,* 10**,** 1131-3.

LI, T., ZHANG, Z., KOLWICZ, S. C., JR., ABELL, L., ROE, N. D., KIM, M., ZHOU, B., CAO, Y., RITTERHOFF, J., GU, H., RAFTERY, D., SUN, H. & TIAN, R. 2017. Defective Branched-Chain Amino Acid Catabolism Disrupts Glucose Metabolism and Sensitizes the Heart to Ischemia-Reperfusion Injury. *Cell Metab,* 25**,** 374-385.

LOPEZ-SORIANO, F. J., FERNANDEZ-LOPEZ, J. A., MAMPEL, T., VILLARROYA, F., IGLESIAS, R. & ALEMANY, M. 1988. Amino acid and glucose uptake by rat brown adipose tissue. Effect of cold-exposure and acclimation. *Biochem J,* 252**,** 843-9.

LU, X., SOLMONSON, A., LODI, A., NOWINSKI, S. M., SENTANDREU, E., RILEY, C. L., MILLS, E. M. & TIZIANI, S. 2017. The early metabolomic response of adipose tissue during acute cold exposure in mice. *Sci Rep,* 7**,** 3455.

LYNCH, C. J. & ADAMS, S. H. 2014. Branched-chain amino acids in metabolic signalling and insulin resistance. *Nat Rev Endocrinol,* 10**,** 723-36.

MADSEN, L., PEDERSEN, L. M., LILLEFOSSE, H. H., FJAERE, E., BRONSTAD, I., HAO, Q., PETERSEN, R. K., HALLENBORG, P., MA, T., DE MATTEIS, R., ARAUJO, P., MERCADER, J., BONET, M. L., HANSEN, J. B., CANNON, B., NEDERGAARD, J., WANG, J., CINTI, S., VOSHOL, P., DOSKELAND, S. O. & KRISTIANSEN, K. 2010. UCP1 induction during recruitment of brown adipocytes in white adipose tissue is dependent on cyclooxygenase activity. *PLoS One,* 5**,** e11391.

MORRISON, S. F. & NAKAMURA, K. 2019. Central Mechanisms for Thermoregulation. *Annu Rev Physiol,* 81**,** 285-308.

NAKAMURA, K. 2011. Central circuitries for body temperature regulation and fever. *Am J Physiol Regul Integr Comp Physiol,* 301**,** R1207-28.

NAKAMURA, K., MATSUMURA, K., KANEKO, T., KOBAYASHI, S., KATOH, H. & NEGISHI, M. 2002. The rostral raphe pallidus nucleus mediates pyrogenic transmission from the preoptic area. *J Neurosci,* 22**,** 4600-10.

NAKAMURA, K. & MORRISON, S. F. 2008. A thermosensory pathway that controls body temperature. *Nat Neurosci,* 11**,** 62-71.

NAKAMURA, K. & MORRISON, S. F. 2011. Central efferent pathways for cold-defensive and febrile shivering. *J Physiol,* 589**,** 3641-58.

NEINAST, M., MURASHIGE, D. & ARANY, Z. 2019a. Branched Chain Amino Acids. *Annu Rev Physiol,* 81**,** 139-164.

NEINAST, M. D., JANG, C., HUI, S., MURASHIGE, D. S., CHU, Q., MORSCHER, R. J., LI, X., ZHAN, L., WHITE, E., ANTHONY, T. G., RABINOWITZ, J. D. & ARANY, Z. 2019b. Quantitative Analysis of the Whole-Body Metabolic Fate of Branched-Chain Amino Acids. *Cell Metab,* 29**,** 417-429 e4.

NEWGARD, C. B., AN, J., BAIN, J. R., MUEHLBAUER, M. J., STEVENS, R. D., LIEN, L. F., HAQQ, A. M., SHAH, S. H., ARLOTTO, M., SLENTZ, C. A., ROCHON, J., GALLUP, D., ILKAYEVA, O., WENNER, B. R., YANCY, W. S., JR., EISENSON, H., MUSANTE, G., SURWIT, R. S., MILLINGTON, D. S., BUTLER, M. D. & SVETKEY, L. P. 2009. A branched-chain amino acid-related metabolic signature that differentiates obese and lean humans and contributes to insulin resistance. *Cell Metab,* 9**,** 311-26.

NORMAN, D. C. 2000. Fever in the elderly. *Clin Infect Dis,* 31**,** 148-51.

OHNO, H., SHINODA, K., SPIEGELMAN, B. M. & KAJIMURA, S. 2012. PPARgamma agonists induce a white-to-brown fat conversion through stabilization of PRDM16 protein. *Cell Metab,* 15**,** 395-404.

OKAMATSU-OGURA, Y., KITAO, N., KIMURA, K. & SAITO, M. 2007. Brown fat UCP1 is not involved in the febrile and thermogenic responses to IL-1beta in mice. *Am J Physiol Endocrinol Metab,* 292**,** E1135-9.

PANIC, V., PEARSON, S., BANKS, J., TIPPETTS, T. S., VELASCO-SILVA, J. N., LEE, S., SIMCOX, J., GEOGHEGAN, G., BENSARD, C. L., VAN RY, T., HOLLAND, W. L., SUMMERS, S. A., COX, J., DUCKER, G. S., RUTTER, J. & VILLANUEVA, C. J. 2020. Mitochondrial pyruvate carrier is required for optimal brown fat thermogenesis. *Elife,* 9.

RILEY, C. L., DAO, C., KENASTON, M. A., MUTO, L., KOHNO, S., NOWINSKI, S. M., SOLMONSON, A. D., PFEIFFER, M., SACK, M. N., LU, Z., FIERMONTE, G., SPRAGUE, J. E. & MILLS, E. M. 2016. The complementary and divergent roles of uncoupling proteins 1 and 3 in thermoregulation. *J Physiol,* 594**,** 7455-7464.

ROBINSON, L. J., LAW, J. M., SYMONDS, M. E. & BUDGE, H. 2016. Brown adipose tissue activation as measured by infrared thermography by mild anticipatory psychological stress in lean healthy females. *Exp Physiol,* 101**,** 549-57.

ROSELL, M., KAFOROU, M., FRONTINI, A., OKOLO, A., CHAN, Y. W., NIKOLOPOULOU, E., MILLERSHIP, S., FENECH, M. E., MACINTYRE, D., TURNER, J. O., MOORE, J. D., BLACKBURN, E., GULLICK, W. J., CINTI, S., MONTANA, G., PARKER, M. G. & CHRISTIAN, M. 2014. Brown and white adipose tissues: intrinsic differences in gene expression and response to cold exposure in mice. *Am J Physiol Endocrinol Metab,* 306**,** E945-64.

SCHELL, J. C., OLSON, K. A., JIANG, L., HAWKINS, A. J., VAN VRANKEN, J. G., XIE, J., EGNATCHIK, R. A., EARL, E. G., DEBERARDINIS, R. J. & RUTTER, J. 2014. A role for the mitochondrial pyruvate carrier as a repressor of the Warburg effect and colon cancer cell growth. *Mol Cell,* 56**,** 400-13.

SCHREIBER, R., DIWOKY, C., SCHOISWOHL, G., FEILER, U., WONGSIRIROJ, N., ABDELLATIF, M., KOLB, D., HOEKS, J., KERSHAW, E. E., SEDEJ, S., SCHRAUWEN, P., HAEMMERLE, G. & ZECHNER, R. 2017. Cold-Induced Thermogenesis Depends on ATGL-Mediated Lipolysis in Cardiac Muscle, but Not Brown Adipose Tissue. *Cell Metab,* 26**,** 753-763 e7.

SHAO, D., VILLET, O., ZHANG, Z., CHOI, S. W., YAN, J., RITTERHOFF, J., GU, H., DJUKOVIC, D., CHRISTODOULOU, D., KOLWICZ, S. C., JR., RAFTERY, D. &

TIAN, R. 2018. Glucose promotes cell growth by suppressing branched-chain amino acid degradation. *Nat Commun,* 9**,** 2935.

SHIN, H., MA, Y., CHANTURIYA, T., CAO, Q., WANG, Y., KADEGOWDA, A. K. G., JACKSON, R., RUMORE, D., XUE, B., SHI, H., GAVRILOVA, O. & YU, L. 2017. Lipolysis in Brown Adipocytes Is Not Essential for Cold-Induced Thermogenesis in Mice. *Cell Metab,* 26**,** 764-777 e5.

SMITH, R. L., SOETERS, M. R., WUST, R. C. I. & HOUTKOOPER, R. H. 2018. Metabolic Flexibility as an Adaptation to Energy Resources and Requirements in Health and Disease. *Endocr Rev,* 39**,** 489-517.

TAJIMA, K., IKEDA, K., CHANG, H. Y., CHANG, C. H., YONESHIRO, T., OGURI, Y., JUN, H., WU, J., ISHIHAMA, Y. & KAJIMURA, S. 2019. Mitochondrial lipoylation integrates age-associated decline in brown fat thermogenesis. *Nat Metab,* 1**,** 886-898.

TOWNSEND, K. L. & TSENG, Y. H. 2014. Brown fat fuel utilization and thermogenesis. *Trends Endocrinol Metab,* 25**,** 168-77.

USHIKUBI, F., SEGI, E., SUGIMOTO, Y., MURATA, T., MATSUOKA, T., KOBAYASHI, T., HIZAKI, H., TUBOI, K., KATSUYAMA, M., ICHIKAWA, A., TANAKA, T., YOSHIDA, N. & NARUMIYA, S. 1998. Impaired febrile response in mice lacking the prostaglandin E receptor subtype EP3. *Nature,* 395**,** 281-4.

VACANTI, N. M., DIVAKARUNI, A. S., GREEN, C. R., PARKER, S. J., HENRY, R. R., CIARALDI, T. P., MURPHY, A. N. & METALLO, C. M. 2014. Regulation of substrate utilization by the mitochondrial pyruvate carrier. *Mol Cell,* 56**,** 425-35.

VEGIOPOULOS, A., MULLER-DECKER, K., STRZODA, D., SCHMITT, I., CHICHELNITSKIY, E., OSTERTAG, A., BERRIEL DIAZ, M., ROZMAN, J., HRABE DE ANGELIS, M., NUSING, R. M., MEYER, C. W., WAHLI, W., KLINGENSPOR, M. & HERZIG, S. 2010. Cyclooxygenase-2 controls energy homeostasis in mice by de novo recruitment of brown adipocytes. *Science,* 328**,** 1158-61.

WALLACE, M., GREEN, C. R., ROBERTS, L. S., LEE, Y. M., MCCARVILLE, J. L., SANCHEZ-GURMACHES, J., MEURS, N., GENGATHARAN, J. M., HOVER, J. D., PHILLIPS, S. A., CIARALDI, T. P., GUERTIN, D. A., CABRALES, P., AYRES, J. S., NOMURA, D. K., LOOMBA, R. & METALLO, C. M. 2018. Enzyme promiscuity drives branched-chain fatty acid synthesis in adipose tissues. *Nat Chem Biol,* 14**,** 1021-1031.

WALTER, E. J., HANNA-JUMMA, S., CARRARETTO, M. & FORNI, L. 2016. The pathophysiological basis and consequences of fever. *Crit Care,* 20**,** 200.

WANG, T. J., LARSON, M. G., VASAN, R. S., CHENG, S., RHEE, E. P., MCCABE, E., LEWIS, G. D., FOX, C. S., JACQUES, P. F., FERNANDEZ, C., O'DONNELL, C. J., CARR, S. A., MOOTHA, V. K., FLOREZ, J. C., SOUZA, A., MELANDER, O., CLISH, C. B. & GERSZTEN, R. E. 2011. Metabolite profiles and the risk of developing diabetes. *Nat Med,* 17**,** 448-53.

WICKS, S. E., VANDANMAGSAR, B., HAYNIE, K. R., FULLER, S. E., WARFEL, J. D., STEPHENS, J. M., WANG, M., HAN, X., ZHANG, J., NOLAND, R. C. & MYNATT, R. L. 2015. Impaired mitochondrial fat oxidation induces adaptive remodeling of muscle metabolism. *Proc Natl Acad Sci U S A,* 112**,** E3300-9.

WU, C., OROZCO, C., BOYER, J., LEGLISE, M., GOODALE, J., BATALOV, S., HODGE, C. L., HAASE, J., JANES, J., HUSS, J. W., 3RD & SU, A. I. 2009. BioGPS: an extensible and customizable portal for querying and organizing gene annotation resources. *Genome Biol,* 10**,** R130.

WURTZ, P., SOININEN, P., KANGAS, A. J., RONNEMAA, T., LEHTIMAKI, T., KAHONEN, M., VIIKARI, J. S., RAITAKARI, O. T. & ALA-KORPELA, M. 2013. Branched-chain and aromatic amino acids are predictors of insulin resistance in young adults. *Diabetes Care,* 36**,** 648-55.

YONESHIRO, T., WANG, Q., TAJIMA, K., MATSUSHITA, M., MAKI, H., IGARASHI, K., DAI, Z., WHITE, P. J., MCGARRAH, R. W., ILKAYEVA, O. R., DELEYE, Y., OGURI, Y., KURODA, M., IKEDA, K., LI, H., UENO, A., OHISHI, M., ISHIKAWA, T., KIM, K., CHEN, Y., SPONTON, C. H., PRADHAN, R. N., MAJD, H., GREINER, V. J., YONESHIRO, M., BROWN, Z., CHONDRONIKOLA, M., TAKAHASHI, H., GOTO, T., KAWADA, T., SIDOSSIS, L., SZOKA, F. C., MCMANUS, M. T., SAITO, M., SOGA, T. & KAJIMURA, S. 2019. BCAA catabolism in brown fat controls energy homeostasis through SLC25A44. *Nature,* 572**,** 614-619.

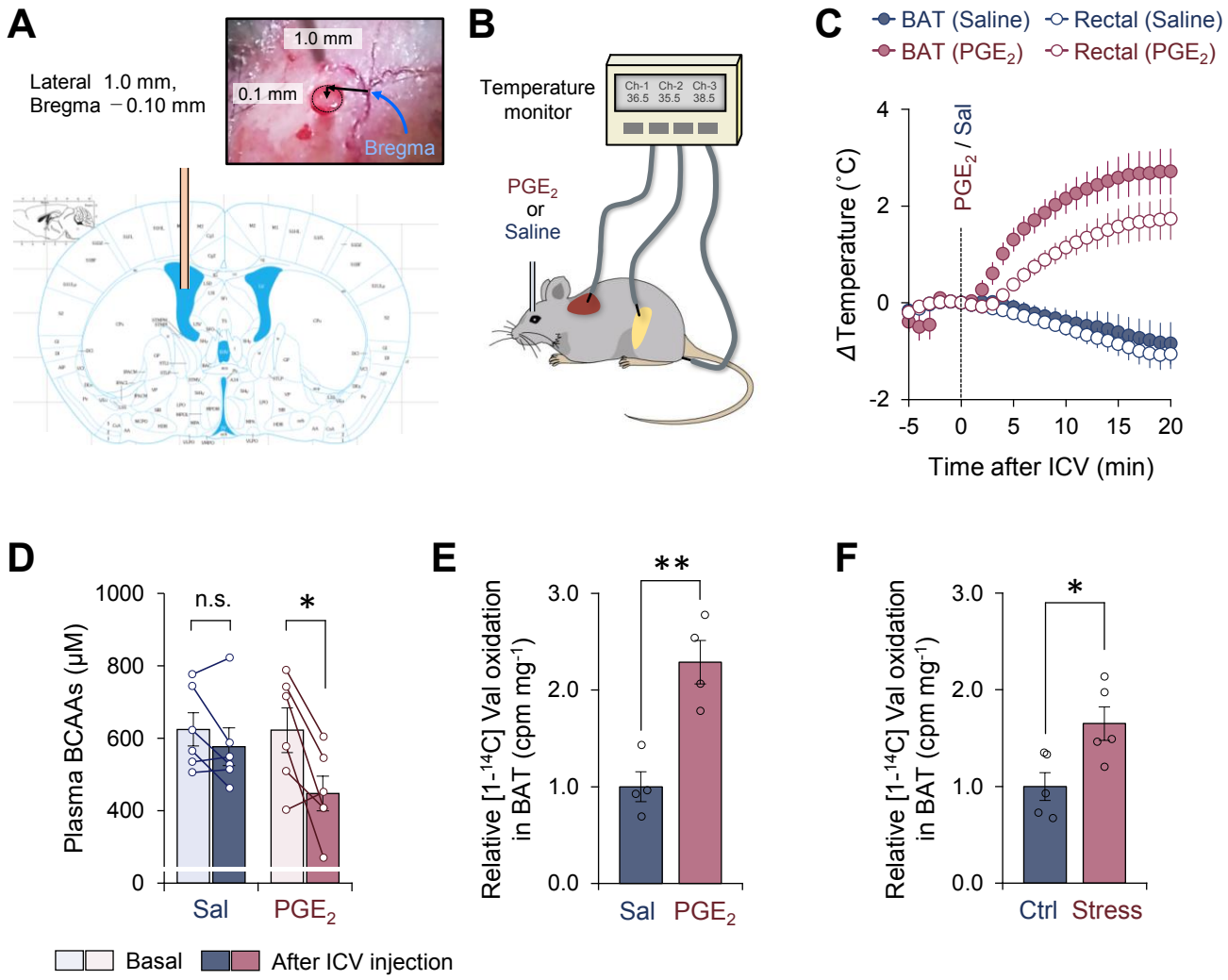

Figure 1. Activation of BCAA catabolism and thermogenesis in the BAT following fever stimuli.

A. The injection site of PGE_2 in the left lateral ventricle. The image was adapted from "The mouse brain in stereotaxic coordinates" (Franklin and Paxinos, 2008).

B. Schematic illustration of the experiment. Mice received intracerebroventricular (ICV) administration of PGE_2 (1.4 μg per mouse) or saline (control). Tissue temperature and rectal temperature were simultaneously recorded by the live monitoring system.

C. Real-time temperature changes in the iBAT and rectum of mice in (B). $n = 6$ per group.

D. Plasma BCAA concentration before and after an ICV administration of PGE_2. $n = 6$ per group.

E. Relative [1-^{14}C] Val oxidation in the iBAT of mice. $n = 4$ per group.

F. Relative [1-^{14}C] Val oxidation in the iBAT of rats exposed to social defeat stress. $n = 5$ per group.

*$P < 0.05$, ** $P < 0.01$, n.s., not significant. Data were analyzed by using paired *t*-test (D) or unpaired Student's *t*-test (E, F).

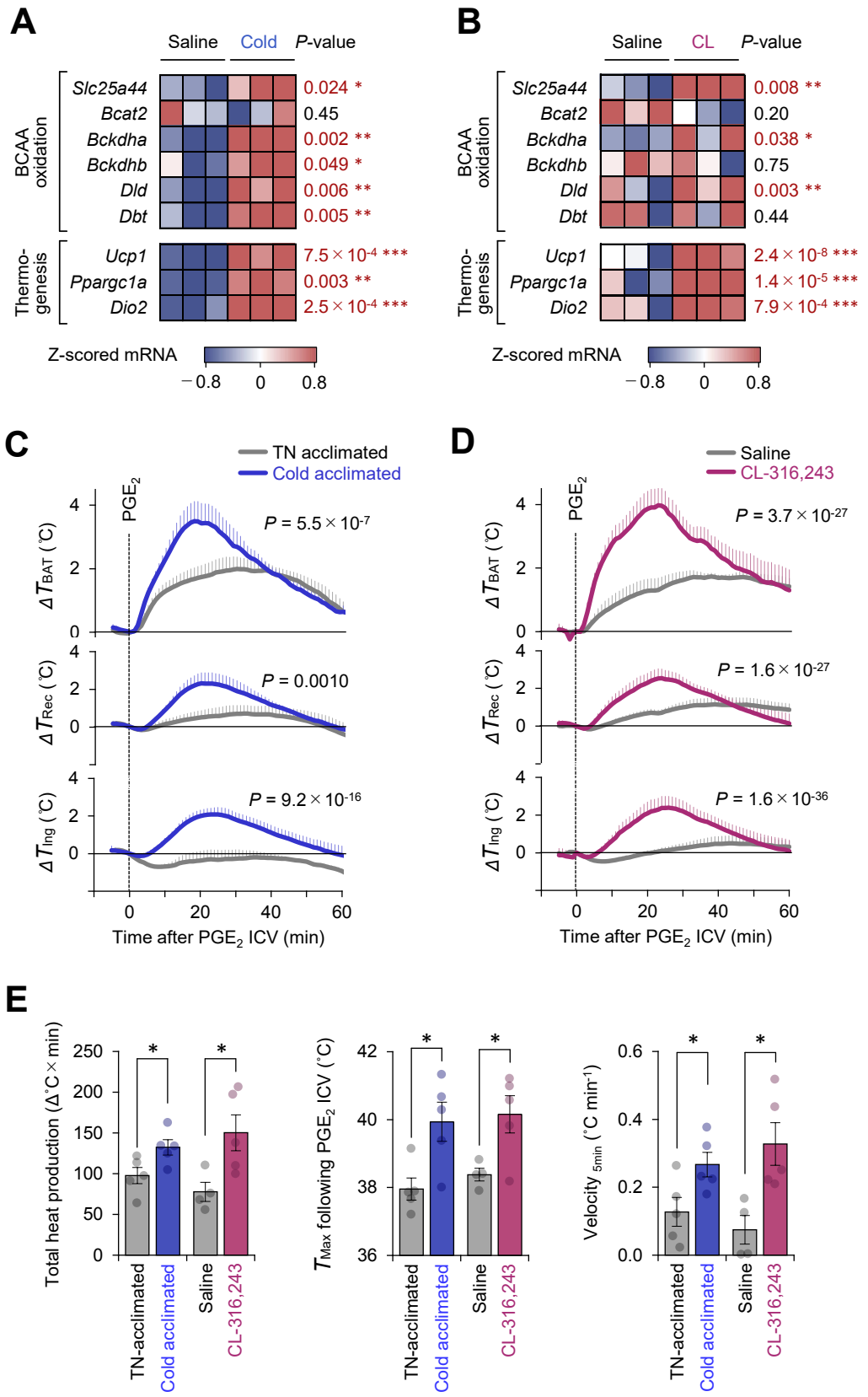

Figure 2

Figure 2. Mitochondrial BCAA catabolism enhances PGE_2-induced fever.

A. mRNA expression of indicated BCAA catabolism genes and thermogenic genes in BAT following cold exposure. $n = 3$ per group. Data were obtained from a previous microarray dataset from GEO under the accession # GSE51080 (Rosell et al., 2014).

B. mRNA expression of indicated BCAA catabolism genes and thermogenic genes in BAT following β_3-AR agonist (CL-316,243; CL) treatment. $n = 3$ per group. Data were obtained from a previous RNA-sequence dataset from ArrayExpress under the accession # E-MTAB-7445(Tajima et al., 2019).

C. Real-time temperature changes in the iBAT (ΔT_{BAT}), rectum (ΔT_{Rec}), and ing-WAT (ΔT_{Ing}) of mice acclimated to thermoneutrality (TN, 30 °C) or cold (15 °C) for 2 weeks. $n = 5$ per group.

D. Real-time temperature changes in the iBAT (ΔT_{BAT}), rectum (ΔT_{Rec}), and ing-WAT (ΔT_{Ing}) of mice treated with β_3-AR agonist (CL-316,243; CL) for 1 week. Saline, $n = 4$; CL, $n = 5$.

E. PGE_2-stimulated total heat production, maximal temperature (T_{Max}), and velocity of tissue temperature in the iBAT of mice in (C) and (D).

Data were analyzed by using unpaired Student's *t*-test (A, B, E) or two-way repeated measures ANOVA (C, D).

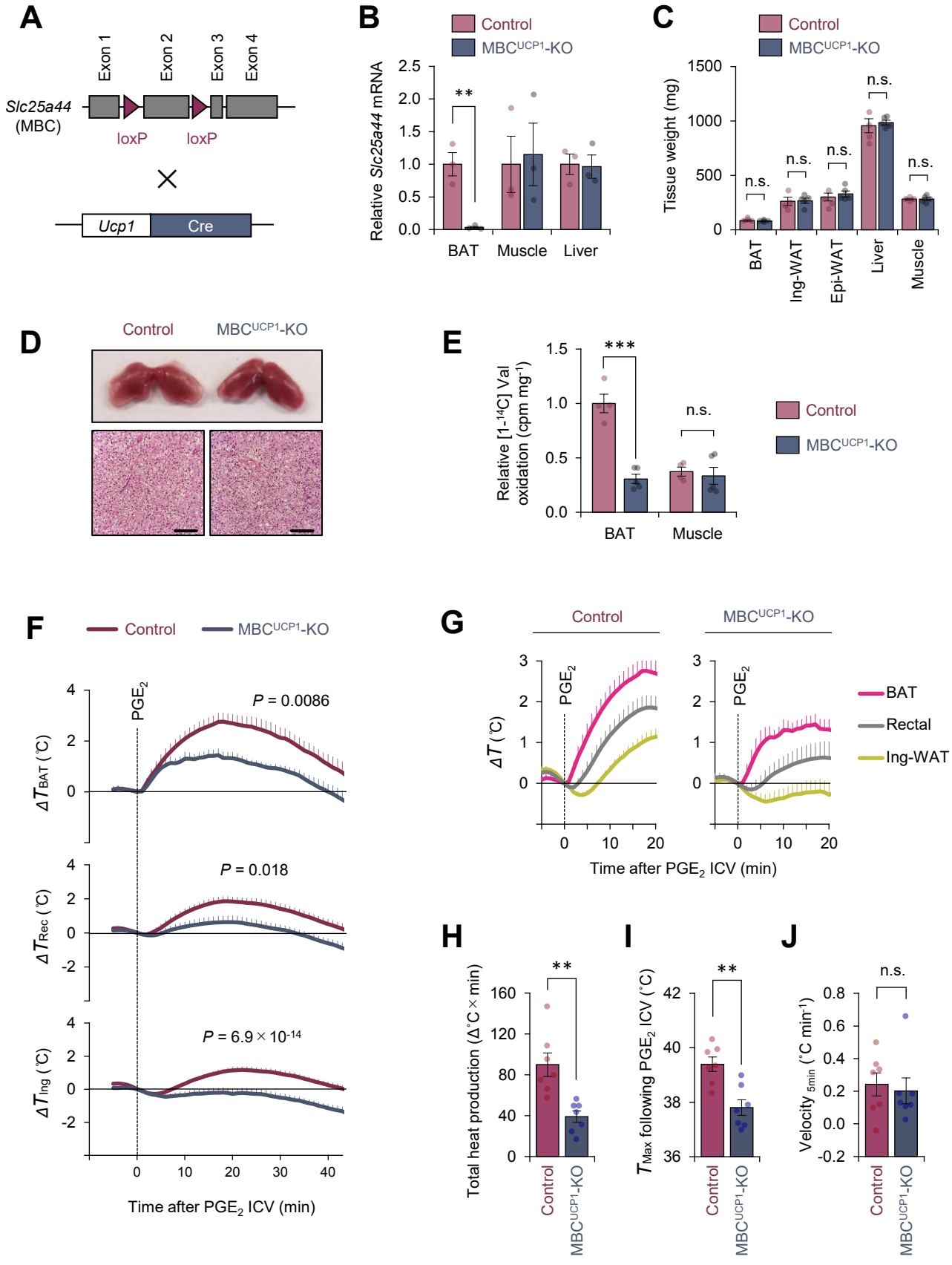

Figure 3

Figure 3. Mitochondrial BCAA carrier SLC25A44/MBC is required for PGE_2-induced fever.

A. Generation of BAT-specific MBC KO mice (*Ucp1*-Cre; *Slc25a44*$^{flox/flox}$; MBC^{UCP1} KO).

B. mRNA expression of *Slc25a44* in the iBAT, skeletal muscle, and liver of BAT-specific MBC KO mice and the littermate control mice. $n = 3$ per group.

C. Tissue weight of the iBAT, ing-WAT, epi-WAT, liver, and gastrocnemius skeletal muscle of BAT-specific MBC KO mice (MBC^{UCP1} KO) and the littermate control mice. Control, $n = 4$; MBC^{UCP1} KO, $n = 5$.

D. Morphology and hematoxylin and eosin (H&E) staining of the iBAT of BAT-specific MBC KO mice and the littermate control mice. Scale bars, 50 μm.

E. Relative [1-^{14}C] Val oxidation in the iBAT and gastrocnemius skeletal muscle of mice in BAT-specific MBC KO mice (MBC^{UCP1} KO) and the littermate control mice. Control, $n = 4$; MBC^{UCP1} KO, $n = 5$.

F. Real-time temperature changes in the iBAT (ΔT_{BAT}), rectum (ΔT_{Rec}), and ing-WAT (ΔT_{Ing}) of BAT-specific MBC KO mice (MBC^{UCP1} KO) and the littermate control mice. $n = 7$ per group.

G. Temperature changes during the first 20 min after ICV administration of PGE_2 in (F).

H. Total heat production in the iBAT following ICV administration of PGE_2 in (F).

I. T_{Max} of iBAT temperature following ICV administration of PGE_2 in (F).

J. Velocity of iBAT temperature increase following ICV administration of PGE_2 in (F).

** $P < 0.01$, *** $P < 0.001$, n.s., not significant. Data were analyzed by using unpaired Student's *t*-test (B, C, E, H-J) or two-way repeated measures ANOVA (F).

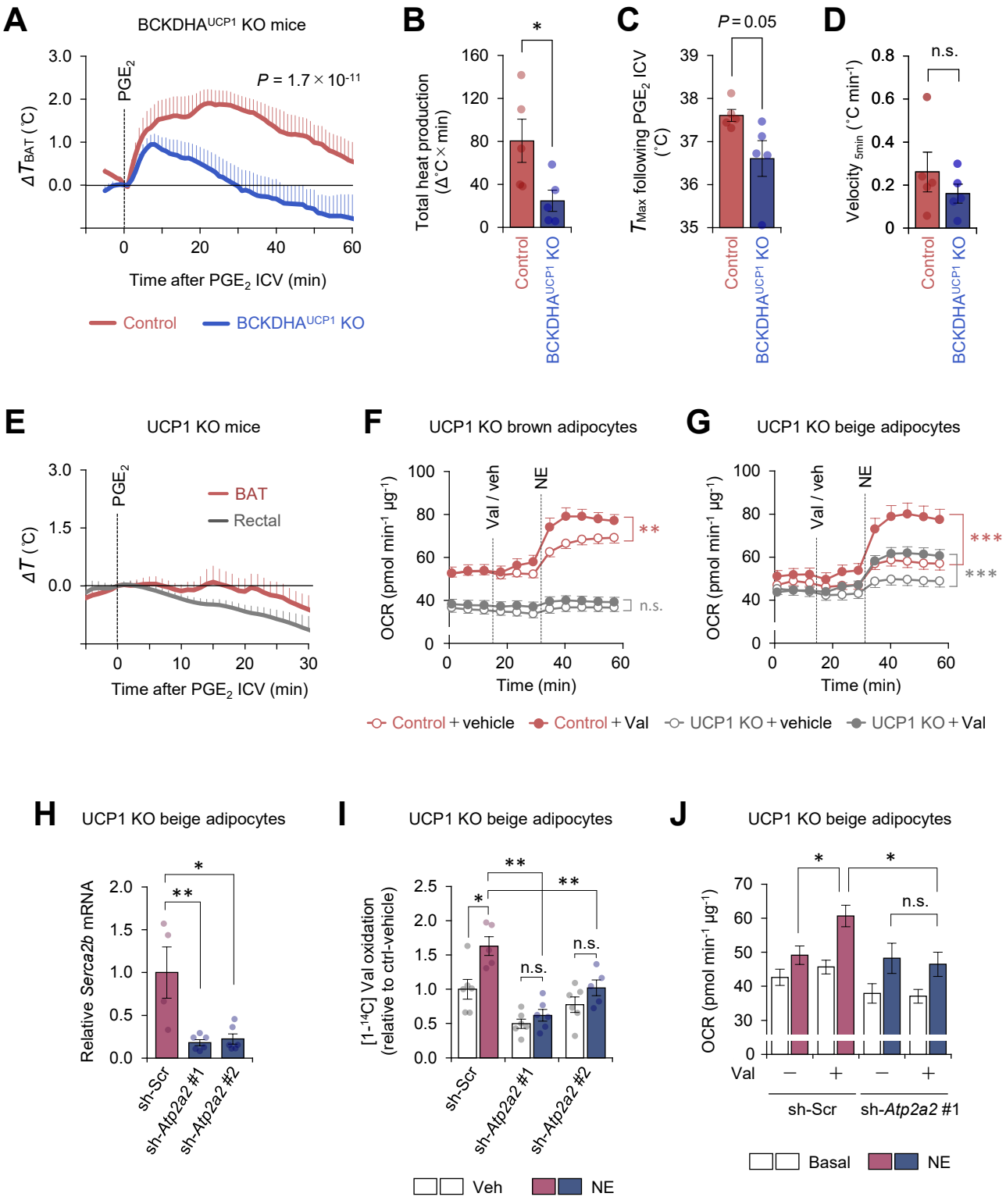

Figure 4

Figure 4. Mitochondrial BCAA oxidation triggers thermogenesis via UCP1-dependent and UCP1-independent mechanisms.

A. Real-time temperature changes in the iBAT of BCKDHA^{UCP1} KO and the littermate control mice following ICV administration of PGE_2. $n = 5$ per group.

B. Total heat production in the iBAT of indicated mice following ICV administration of PGE_2 in (A).

C. T_{max} of iBAT temperature following ICV administration of PGE_2 in (A).

D. Velocity of iBAT temperature increase following ICV administration of PGE_2 in (A).

E. Real-time temperature changes in the iBAT and rectum of UCP1 KO mice following ICV injection of PGE_2. $n = 5$ per group.

F. Oxygen consumption rate (OCR) in brown adipocytes derived from wild-type mice (control) or UCP1 KO mice. Differentiated adipocytes in the BCAA-free medium were treated with valine (Val) or vehicle (Veh), and subsequently stimulated with norepinephrine (NE) at indicated time points. OCR values were normalized by total protein (μg). $n = 10$ per group.

G. OCR in beige adipocytes derived from wild-type mice (control) or UCP1 KO mice. Differentiated adipocytes in the BCAA-free medium were treated with valine (Val) or vehicle (Veh), and subsequently stimulated with norepinephrine (NE) at indicated time points. OCR values were normalized by total protein (μg). Control + vehicle, $n = 9$; Control + Val $n = 8$; UCP1 KO + vehicle, $n = 6$; UCP1 KO + Val, $n = 9$.

H. mRNA expression of *Serca2b* in UCP1 KO beige adipocytes expressing a scrambled control (Scr, $n = 4$) or two independent shRNAs targeting *Atp2a2* (#1 and #2, $n = 6$ per group).

I. Relative [1-^{14}C] Val oxidation in UCP1 KO beige adipocytes in (H). Differentiated adipocytes were cultured in the presence of NE or vehicle. Valine oxidation was measured using [1-^{14}C] valine and normalized by total protein (μg). Vehicle $n = 6$, NE $n = 5$, except sh-*Atp2a2* #1 treated with NE $n = 6$.

J. OCR was measured in UCP1 KO beige adipocytes in (H). Differentiated adipocytes were incubated in the BCAA-free media supplemented with Val (sh-Scr, $n = 9$; sh-*Atp2a2*, $n = 6$) or vehicle (sh-Scr, $n = 6$; sh-*Atp2a2*, $n = 7$), and subsequently stimulated with NE. OCR values were normalized by total protein (μg).

* $P < 0.05$, ** $P < 0.01$, *** $P < 0.001$, n.s. not significant. Data were analyzed by unpaired Student's *t*-test (B-D), one- (H) or two-way (I) factorial ANOVA followed by Tukey's post hoc test, or two-way repeated measures ANOVA (A, F, G) followed by Tukey's post hoc test (J).

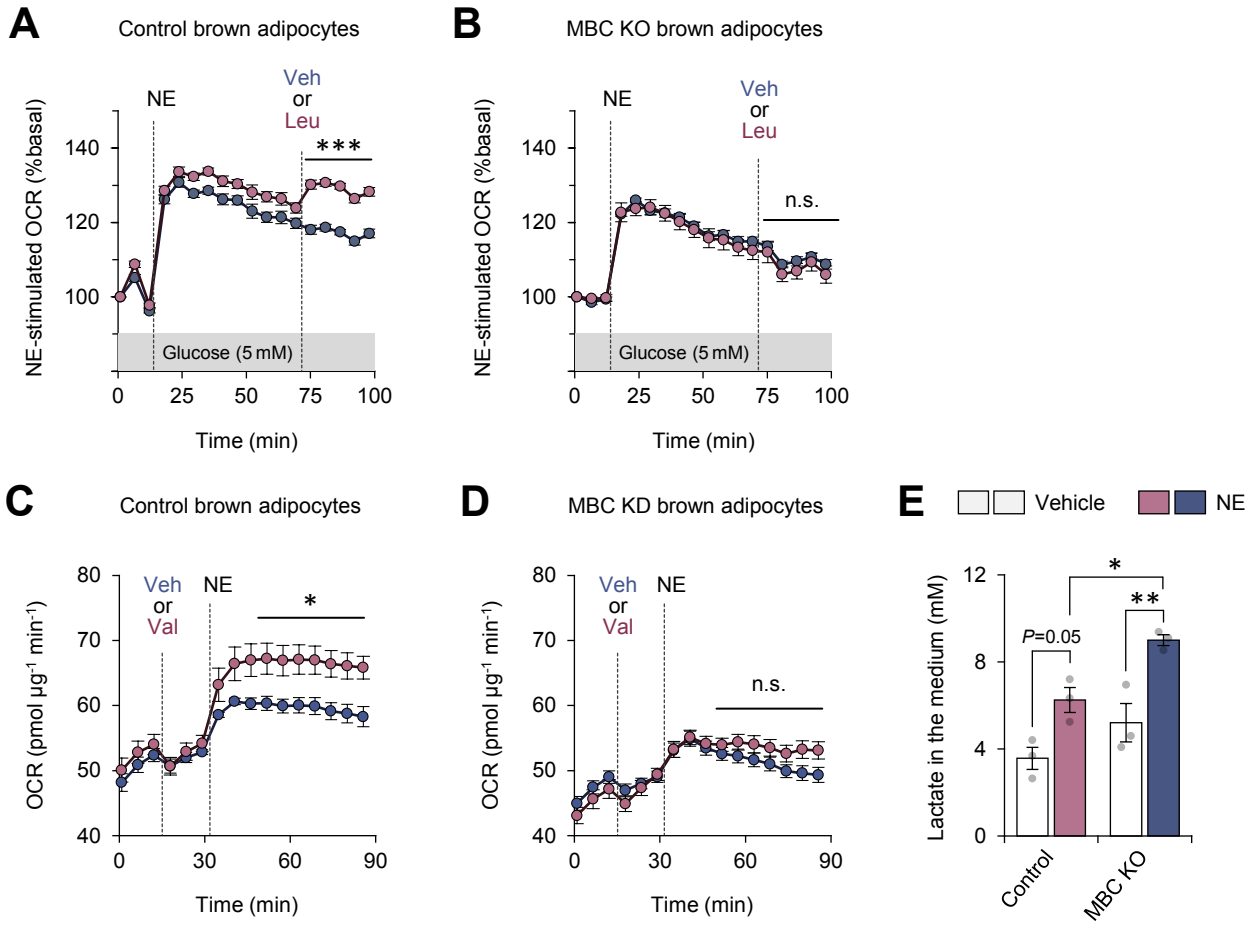

Figure 5. Mitochondrial BCAA catabolism required for sustained thermogenesis.

A. Oxygen consumption rate (OCR) normalized to total protein (in µg) in control brown adipocytes. Differentiated adipocytes in BCAA-free medium with 5 mM glucose were stimulated with norepinephrine (NE), and subsequently supplemented with Leu or vehicle. $n = 9$ per group.

B. OCR normalized to total protein (in µg) in MBC KO brown adipocytes. Differentiated adipocytes cultured in BCAA-free medium with glucose (5 mM) were stimulated with NE, and subsequently supplemented with Leu or vehicle. $n = 9$ per group.

C. OCR normalized to total protein (in µg) in control brown adipocytes. Differentiated adipocytes in BCAA-free medium with glucose (20 mM) were supplemented with Val or vehicle, and subsequently stimulated with NE. $n = 5$ per group.

D. OCR normalized to total protein (in µg) in MBC KO brown adipocytes. Differentiated adipocytes in BCAA-free medium with glucose (20 mM) were supplemented with Leu or vehicle, and subsequently stimulated with NE. $n = 5$ per group.

E. Lactate production in control and MBC KO brown adipocytes. Differentiated adipocytes were stimulated with vehicle or NE for 30 min, and lactate content in the medium was measured. $n = 3$ per group.

* $P < 0.05$, ** $P < 0.01$, *** $P < 0.001$, n.s. not significant. Data were analyzed by two-way repeated measures ANOVA (A-D) or two-way factorial ANOVA followed by Tukey's post hoc test (E).

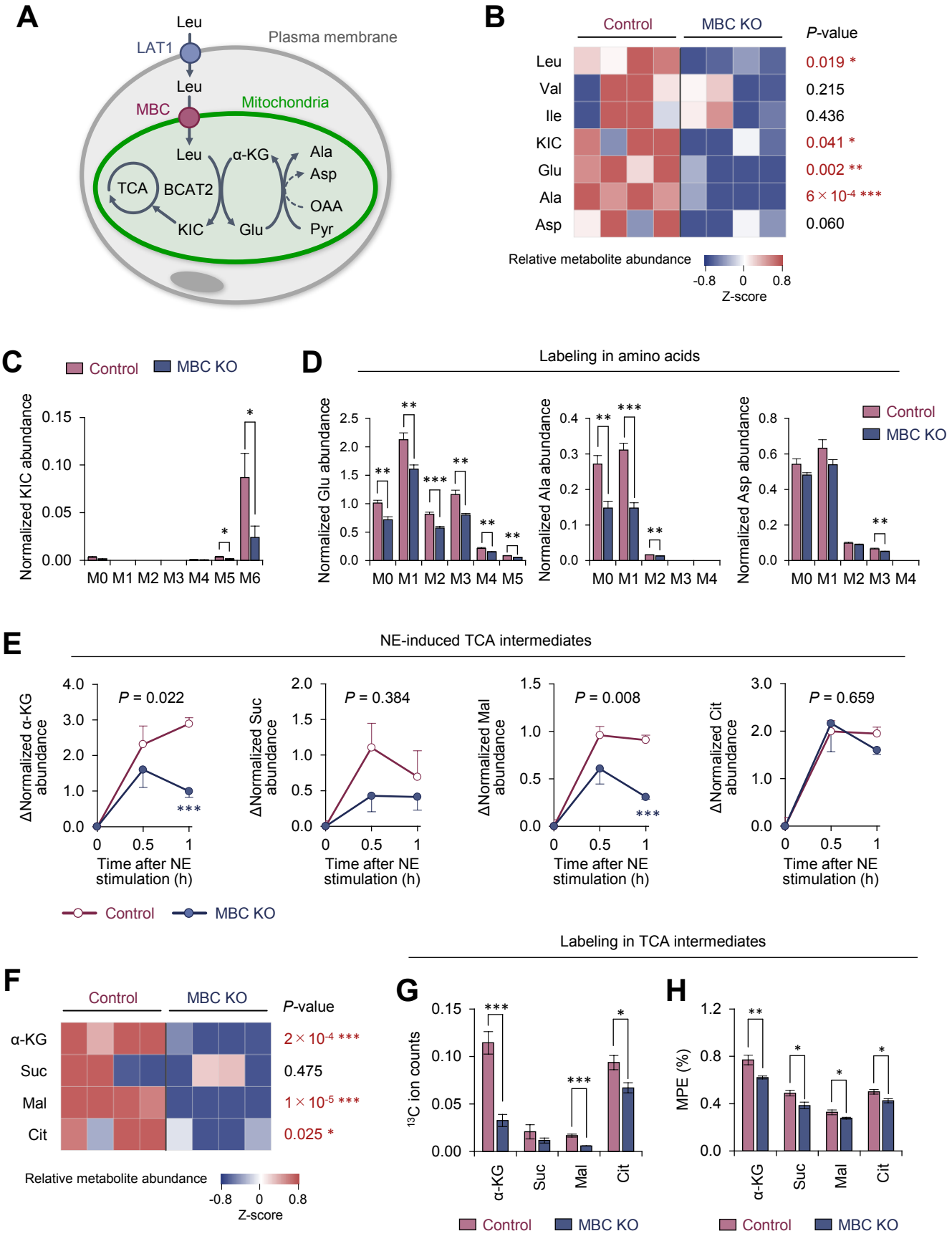

Figure 6

Figure 6. MBC is required for the synthesis of the mitochondrial amino acids and TCA intermediates.

A. Schematic illustration of mitochondrial BCAA fate to the TCA cycle and amino acid synthesis.

B. Amino acid relative abundance in WT control and MBC KO brown adipocytes as determined by ^{13}C-Leu metabolomics. Cells were harvested at a basal state. $n = 4$ per group.

C. Leu-derived ^{13}C labeling in KIC in wild type control and MBC KO brown adipocytes in (B).

D. Labeling in indicated amino acids derived from Leu in WT control and MBC KO brown adipocytes in (B).

E. NE-induced changes in TCA cycle intermediates in WT control and MBC KO brown adipocytes. Cells were harvested at the indicated time points following norepinephrine (NE) treatment in (B).

F. The relative abundance of indicated TCA cycle intermediate in WT control and MBC KO brown adipocytes at one hour following norepinephrine (NE) treatment in (B).

G. Leu-derived ^{13}C labeling in TCA cycle intermediates in WT control and MBC KO brown adipocytes. Cells were harvested at one hour following norepinephrine (NE) treatment in (B).

H. Mole percentage enrichment (MPE) of TCA cycle intermediates derived from [U-$^{13}C_6$] Leu in control and MBC KO brown adipocytes. Cells were harvested at one hour following norepinephrine (NE) treatment. $n = 4$ per group.

Data in 6B-H was normalized to a norvaline internal standard. * $P < 0.05$, ** $P < 0.01$, *** $P < 0.001$. Data were analyzed by unpaired Student's *t*-test (B-D, F-H) or two-way factorial ANOVA followed by post hoc unpaired *t*-test.

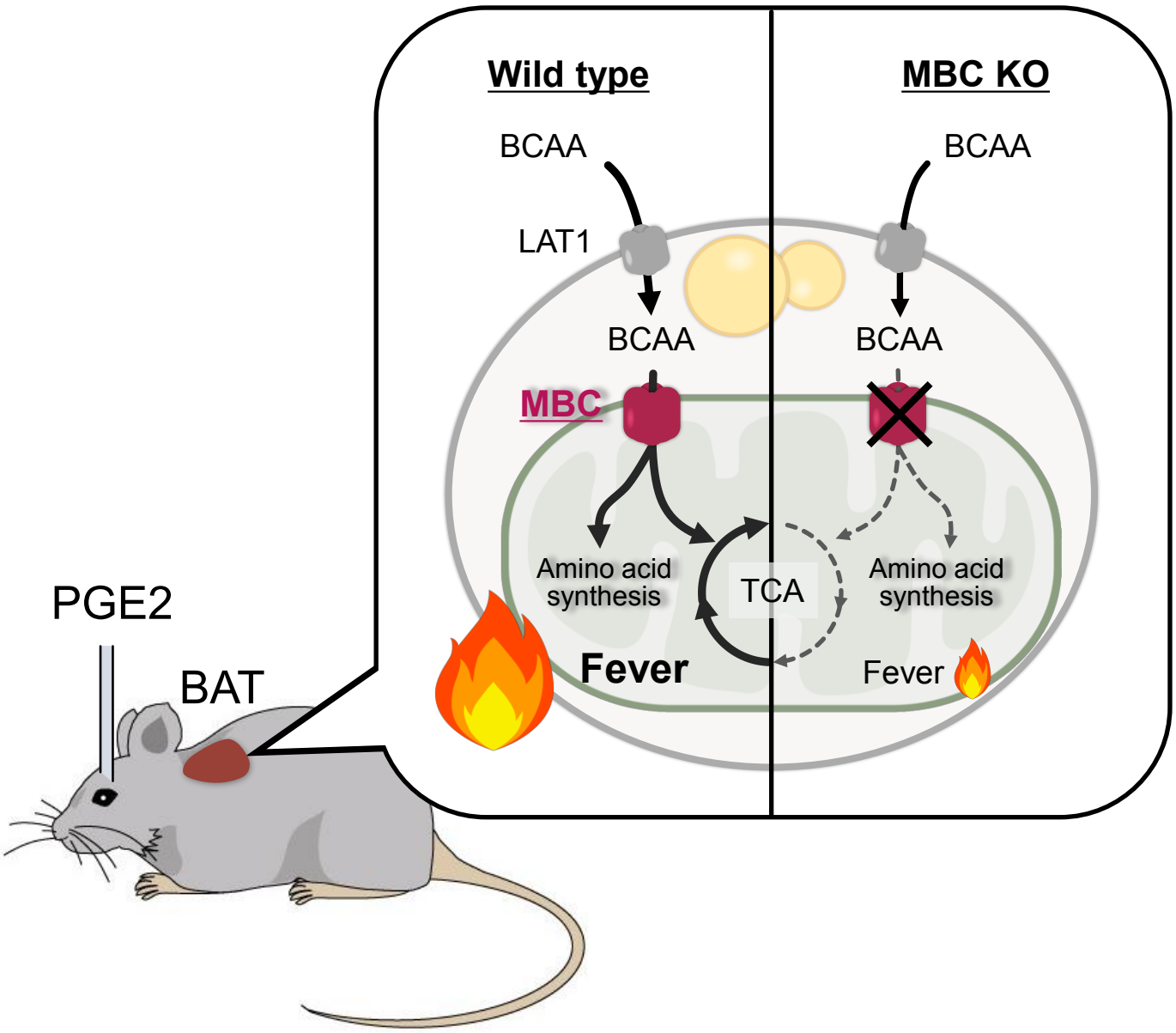

Figure 7. A model of mitochondrial BCAA catabolism and BAT thermogenesis in response to fever stimuli.

In response to ICV administration of PGE_2 or psychological stress, mitochondrial BCAA catabolism in the BAT is activated along with enhanced thermogenesis. The fever-induced mitochondrial BCAA catabolism is required for sustaining thermogenesis. Mitochondrial BCAA uptake via MBC is required for BCAA deamination and the synthesis of mitochondrial amino acid pool and TCA intermediates.

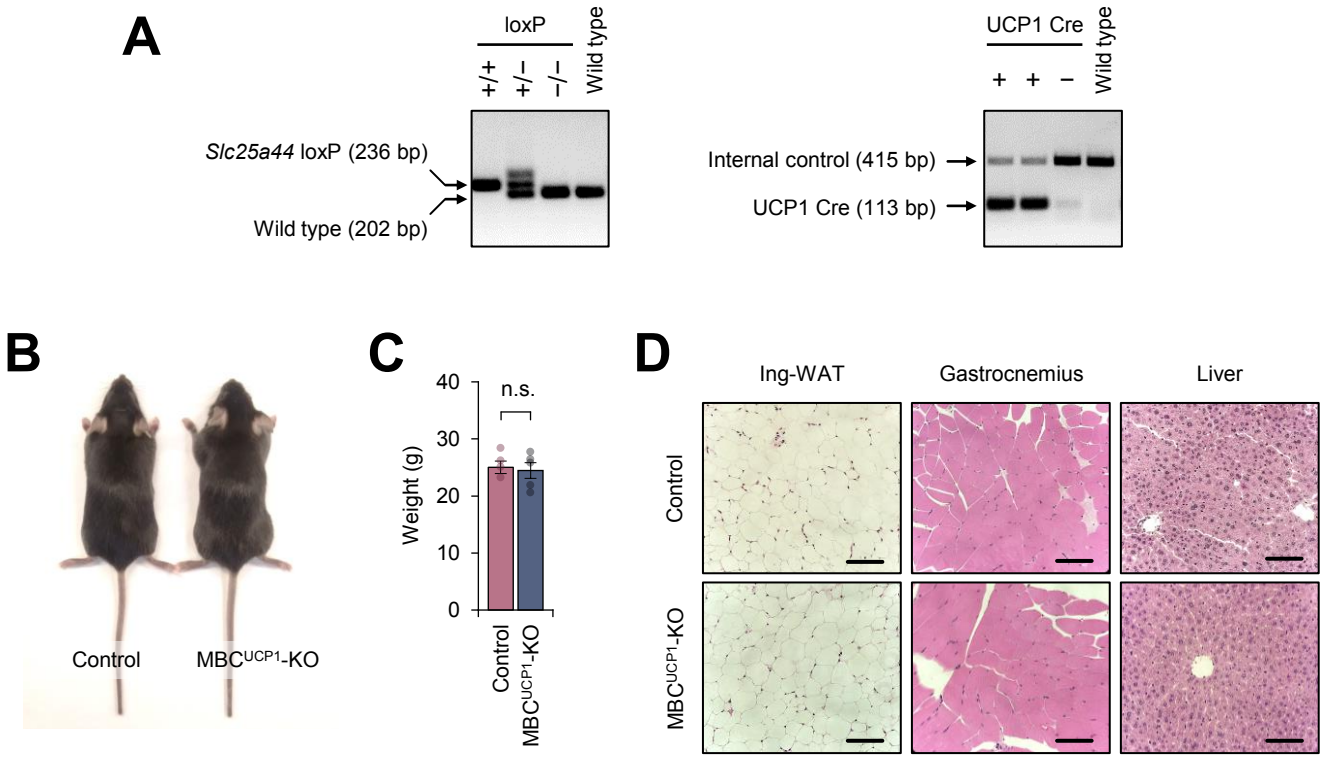

Supplemental Figure 1. Characterization of BAT-specific MBC KO mice.

A. Representative genotyping images of BAT-specific MBC KO mice (*Ucp1*-Cre x *Slc25a44*$^{flox/flox}$; MBC^{UCP1} KO) and the littermate control mice (*Slc25a44*$^{flox/flox}$).

B. A representative picture of BAT-specific MBC KO mouse and littermate control mouse.

C. Body weight of BAT-specific MBC KO mice and littermate control mice on a regular chow diet. Control, $n = 4$; MBC^{UCP1} KO, $n = 5$. n.s., not significant by unpaired Student's *t*-test.

D. H&E staining of the ing-WAT, gastrocnemius skeletal muscle, and liver of BAT-specific MBC KO mice and littermate control mice in (C).

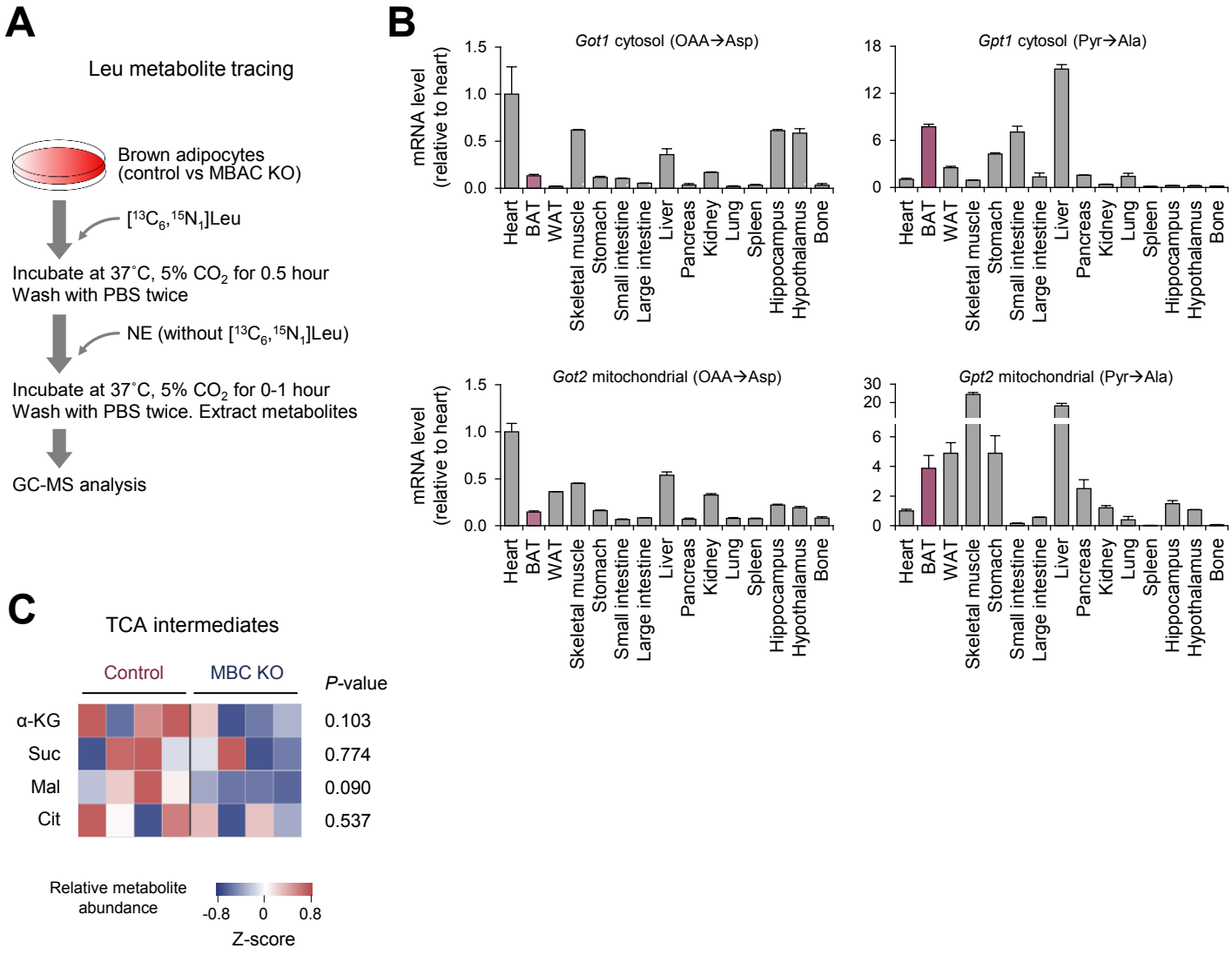

Supplemental Figure 2. Metabolic fate of Leu in MBC KO brown adipocytes.

A. Schematic protocol of Leu metabolite tracing experiment.

B. Tissue distribution of indicated genes that are involved in amino acid synthesis from BCAA. Glutamate-pyruvate transaminase (GPT), the cytoplasmic form (Gpt1) and the mitochondrial form (Gpt2), catalyze the reversible conversion of Ala and α-KG to Glu and pyruvate. Aspartate aminotransferase (GOT), the cytoplasmic form (Got1) and the mitochondrial form (Got2) catalyze the interconversion of Asp and oxaloacetate (OAA). The data are derived from BioGPS (Wu et al., 2009).

C. The relative abundance of indicated TCA cycle intermediate in WT control and MBC KO brown adipocytes at a basal condition. $n = 4$ per group.

Supplemental Table 1. Primer sequences

Gene	Forward primer	Reverse primer
Slc25a44	TCGCTGCTAACGTACATCCC	AGACAATGTGAGGGCACTCC
Serca2b	ACCTTTGCCGCTCATTTTCCAG	AGGCTGCACACACTCTTTACC
36B4	GGCCCTGCACTCTCGCTTTC	TGCCAGGACGCGCTTGT